

OPTICS OF LIQUID CRYSTALS

PACS numbers: 78.15.+e; 78.60.Lc; 78.67.Pt; 42.70.Df
DOI: 10.1070/QE2013v043n11ABEH015280

Angular dependences of the luminescence and density of photon states in a chiral liquid crystal

B.A. Umanskii, L.M. Blinov, S.P. Palto

Abstract. **Luminescence spectra of a laser dye-doped chiral liquid crystal have been studied in a wide range of angles (up to 60°) to the axis of its helical structure using a semicylindrical quartz prism, which made it possible to observe the shift and evolution of the photonic band gap in response to changes in angle. Using measured spectra and numerical simulation, we calculated the spectral distributions of the density of photon states in such a cholesteric crystal for polarised and unpolarised light, which characterise its structure as that of a chiral one-dimensional photonic crystal.**

Keywords: *luminescence, photonics, chiral liquid crystals.*

1. Introduction

Chiral liquid crystals (CLCs) possess unique optical properties [1, 2] and are being used increasingly in display devices, photonic structures and microlasers [3]. The CLC laser output frequency and polarisation can be tuned readily by varying the composition of the material, as well as by external influences, such as temperature, mechanical stress or electric field [4]. Owing to their periodic, helical structure, CLCs are also of great interest for theoretical studies of the density of photon states, which is responsible for the spectral characteristics of light amplification and lasing [5]. In this context, spectral studies of luminescence in CLCs are of considerable importance because they enable one to calculate the density of states (DOS) [6, 7].

One important issue pertaining to the DOS in CLCs is experimental studies of their optical properties not only along the z axis of the cholesteric helix but also at various angles to this direction. Detailed measurements of reflection spectra at various angles to the z axis were made by Takezoe et al. [8], and very recently lasing was observed at large angles to the helix axis [9, 10]. At the same time, luminescence without amplification is needed to quantitatively estimate the DOS in a wide angular range, which requires a special experimental procedure. This issue is addressed in this report.

2. Experimental

A key component of the chiral material studied was the well-known nematic mixture E7 (Merck). Its ordinary (n_o) and extraordinary (n_e) refractive indices are indicated in Table 1 (these values were used in modelling the transmission spectra of our samples at different angles of incidence of light). A chiral material [3.68 wt % 1,4:3,6-dianhydro-D-sorbitol-2,5-bis(4-hexyloxybenzoate)] was added to E7, which ensured a helix pitch $P_0 = 0.527$ μm and a band gap of the chiral mixture between 800 and 920 nm for light propagating along the helix axis [Fig. 1, spectrum (*1*)]. At the photonic band edges, we observed transmission oscillations, so-called band-edge modes [11], indicative of a good degree of orientational order in the CLC. The dimethylaminonitrostilbene (DMANS) laser dye (0.7%) was added to the chiral mixture. Its absorption spectrum in the range 370–560 nm enabled luminescence excitation by 405- and 532-nm laser diodes. At the same time, we were able to observe the luminescence spectrum of DMANS in the range 480–800 nm [Fig. 1, spectrum (*2*)] at large angles to the helix axis in the region of the band gap, which rapidly shifted to shorter wavelengths with increasing observation angle.

Table 1. Refractive indices of E7 at particular wavelengths.

Index	λ/nm			
	436	509	577	644
n_o	1.544	1.5311	1.523	1.5175
n_e	1.821	1.7737	1.75	1.7354
$\langle n \rangle$	1.6825	1.6524	1.6365	1.6264

The dye-containing chiral mixture was drawn by capillary forces into the gap of a cell formed by a glass plate and semicylindrical quartz prism. The inner surfaces of the glass and quartz were coated with polyimide layers and rubbed with

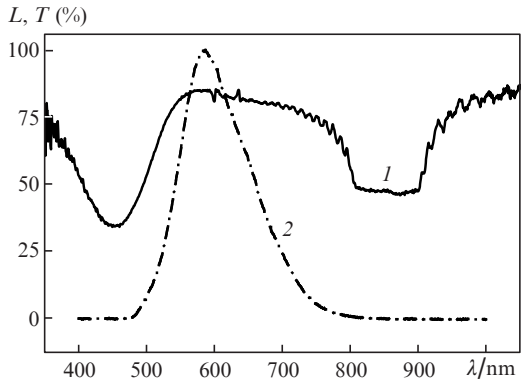

Figure 1. (*1*) Transmission (T) and (*2*) normalised luminescence (L) spectra of a 13-μm-thick layer of the chiral mixture.

B.A. Umanskii, L.M. Blinov, S.P. Palto A.V. Shubnikov Institute of Crystallography, Russian Academy of Sciences, Leninsky prosp. 59, 119333 Moscow, Russia; e-mail: umanskii@yahoo.com, palto@hotmail.ru

Received 13 July 2013; revision received 31 July 2013
Kvantovaya Elektronika **43** (11) 1078–1081 (2013)
Translated by O.M. Tsarev

cloth to uniformly align the long molecular axes (director) of the CLC on the surfaces along the x axis and align the helix axis in the bulk along the z axis (Fig. 2). The cell gap was set by Teflon spacers, which thus determined the thickness of the liquid-crystal layer: 21 and 13 μm in two samples studied. The emission from the dye was excited by a thin laser diode beam (20–50 mW) parallel to the z axis. The luminescence spectrum was measured using an Avantes-2048 spectrometer through fibre-optic cable, which was secured on a stage with a scale, capable of rotating in the xy plane together with a filter, polariser and quarter-wave plate (Fig. 2). The experimental setup allowed us to rotate the pupil of the fibre through an angle $\alpha \leqslant 72°$, ensuring a maximum internal angle in the CLC $\beta \leqslant 58°$, as follows from Snell's law, $\sin\alpha = (\langle n\rangle/n_q)\sin\beta$, at the refractive indices of the quartz prism, $n_q = 1.458$, and CLC, $\langle n\rangle = 1.636$, in the spectral range of the luminescence (Table 1).

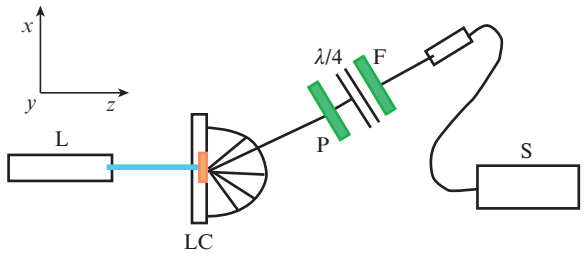

Figure 2. Schematic of the experimental setup (top view): L, laser; LC, liquid-crystal cell; S, spectrometer; P, polariser; F, filter; λ/4, quarter-wave plate.

3. Luminescence measurements

First, we determined the position of the band edges in the luminescence spectrum at a varied external angle α and compared the results to the position of the band gap in transmission spectra, which are easy to model using parameters of the CLC (Fig. 3). In simulation, we used an algorithm developed earlier by exactly solving Maxwell's equations for layered media using Berreman 4 × 4 matrices [12, 13]. A Berreman matrix allows one to examine the transmission and reflection of light waves in a medium with continuously varying parameters at an arbitrary angle of incidence, with allowance for multiple reflection interference. The algorithm was described in great detail elsewhere [12], using several liquid crystals as examples. The experimentally determined positions of the longer (λ_e) and shorter (λ_o) wavelength band edges in Fig. 3 were extracted from right circularly polarised luminescence spectra. The curves were obtained by simulating light transmission (also for a right circularly polarised wave) using wavelength-dependent indices of refraction (Table 1), a helix pitch $P_0 = 0.5259$ and a CLC layer thickness $d = 21$ μm (40 helix turns). The CLC was taken to be situated in a medium whose refractive index was equal to its average refractive index, $\langle n\rangle = 1.626$, which ruled out unwanted reflections from the boundaries of the layer. It is worth noting good agreement between the experimental data and simulated transmission.

Figure 4a shows a typical right circularly polarised luminescence spectrum in the region of the band gap at an external angle $\alpha = 48°$ (solid line). There is a well-defined characteristic dip at the centre of the band gap, corresponding to the contribution of the left circularly polarised component, which was discussed in detail previously in the context of spectral reflection measurements [8]. Spectrum (*2*) corresponds to the right circularly polarised luminescence spectrum measured at zero observation angle, so that the band gap lies beyond the spectrum (Fig. 1). Note that this spectrum is essentially identical in shape to that of the DMANS dye in the nematic (untwisted) liquid crystal E7. For this reason, spectrum (*2*) can be used to normalise the luminescence spectrum and calculate the DOS spectrum. It is the ratio of spectra (*1*) and (*2*) that gives the DOS (ρ) spectrum in Fig. 4b, with $\rho = 1$ corresponding to the luminescence of a uniform layer of a hypothetical CLC with

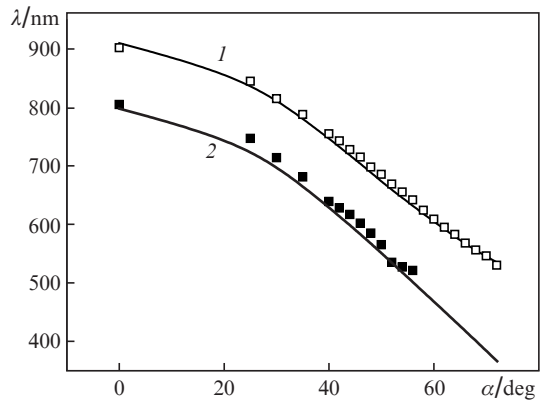

Figure 3. Spectral position of the (*1*) longer and (*2*) shorter wavelength band edges vs. observation angle: experimental data (squares) and simulation results (solid lines).

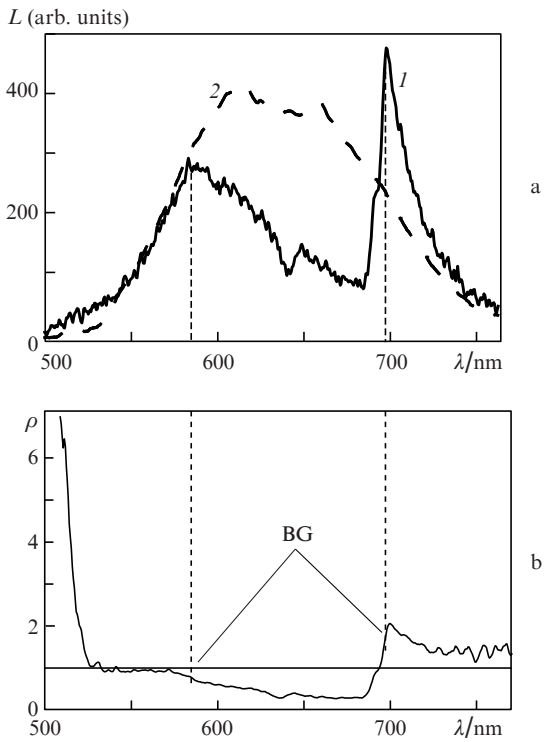

Figure 4. (a) Right circularly polarised luminescence spectra of the CLC at α = (*1*) 48° and (*2*) 0; (b) DOS (ρ) spectrum (in units of $\langle n\rangle/c_0$) of the CLC at α = 48°. The vertical dashed lines indicate the band gap (BG).

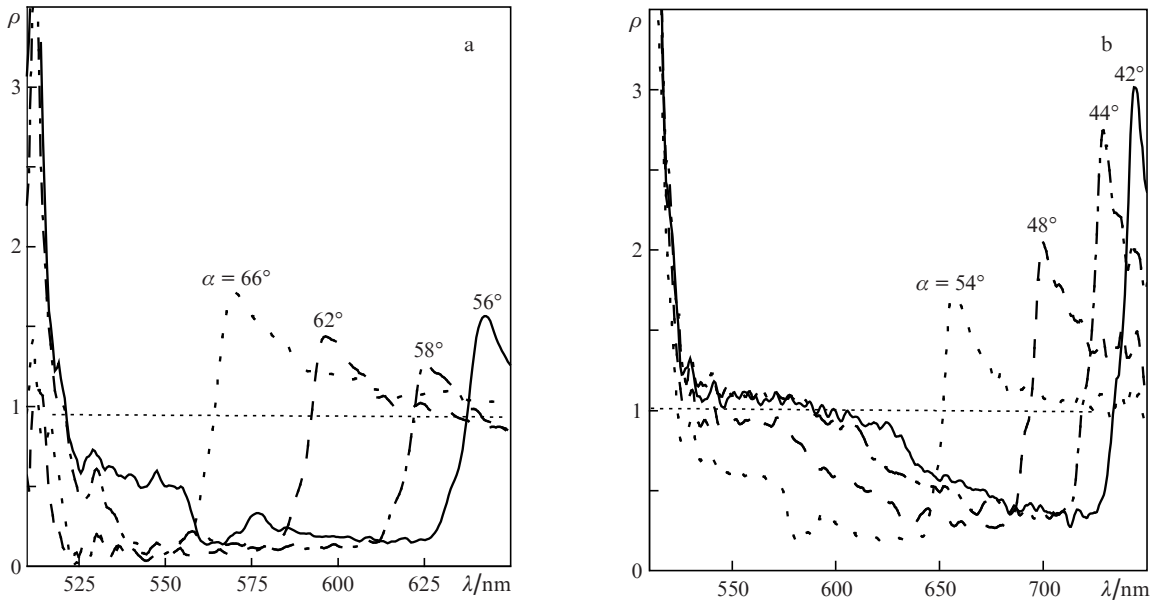

Figure 5. DOS (ρ) spectra for right circularly polarised light at external angles between the luminescence beam and cholesteric helix axis (a) α = 56–66° and (b) α = 42–54°.

no helix. Absolute ρ values can be obtained by multiplying the values plotted on the vertical axis by $\langle n\rangle/c_0 = 5.417\times10^{-9}$ s m^{-1}, where $\langle n\rangle = 1.625$ and c_0 is the speed of light in vacuum [6, 7].

4. Angular dependences of ρ spectra and discussion

To save space, Fig. 5 presents main measured DOS spectra of a 21-μm-thick sample for only the right circularly polarised component, where $\rho \sim 0$ in the region of the band gap. Even though no dependences are presented for unpolarised light, note that, at small angles (α = 30–59°), the band gap bottom lies at a level of ρ = 0.5, but increasing the angle produces dips, down to ~0.2 at α = 62°, due to the transmission of left circularly polarised light.

Figure 6 presents maximum ρ values for unpolarised light [curve (*2*)] and for the right circularly polarised component [curve (*1*), derived from the data in Fig. 5]. In Fig. 6, there is a pronounced tendency for the maximum DOS value to decrease with increasing α. Experimental studies of polarised luminescence along the helix axis (α = 0) yielded $\rho_{max} \sim 5$ [6] at a cell thickness (d = 22 μm) almost identical to that in this study. Extrapolating the curves in Fig. 6 to α = 0, we obtain $\rho_{max} \sim 5$–6 in the angular range 0–20°. Note that direct calculation of the density of states along the axis of an ideal helix (with no absorption or scattering loss) with the use of complex transmittance [14] gives $\rho \sim 20$ at α = 0 and d = 20 μm. The considerable discrepancy between the experimental data and theoretical predictions can be accounted for by the difference in losses and, particularly, by the CLC's domain structure produced during cell fabrication.

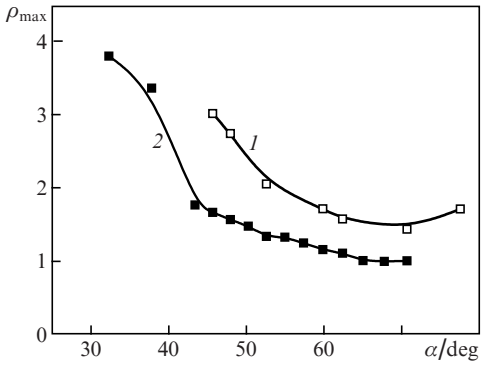

Figure 6. Angular dependences of the maximum DOS value ρ_{max} for (*1*) right circularly polarised and (*2*) unpolarised light.

One question to be answered in this context is why the DOS decreases with increasing luminescence output angle. To the best of our knowledge, there are no theoretical approaches for calculating such spectra except when light propagates along the helix axis of a CLC [6, 14]. For this reason, we present simple estimates of angle-dependent ρ with the use of an approach [15] based on the uncertainty relation $\Delta\omega\Delta\tau \approx 2$ between the width $\Delta\omega$ of Lorentzian band-edge modes and their dwell time $\Delta\tau$ in a cavity. Knowing the spectral mode width $\Delta\lambda$ in the bulk of the CLC, we obtain

$$\Delta\omega = 2\pi c_0\Delta\lambda/\langle n\rangle\lambda^2, \tag{1}$$

$$\rho = \frac{\partial k(\omega)}{\partial\omega} = \frac{1}{v_g} = \frac{\tau}{d} = \frac{2}{d\Delta\omega}. \tag{2}$$

Here, k and v_g are the wave vector and group velocity of light in a CLC layer. The validity of this approach was verified by comparing the ρ values obtained with the above formula at α = 0 and those calculated with the use of complex transmittance at zero angle [14]. Moreover, since band-edge modes are well seen in simulated angle-dependent transmission spectra, in contrast to those in experiments, their spectral width $\Delta\lambda$, roughly equal to the mode spacing, can be estimated from the number of modes, N, in a particular $\Delta\Lambda$ range, e.g. $\Delta\Lambda \sim$ 20 nm. The angular dependence of $\rho = \lambda^2/(\pi d\Delta\lambda)$ (in units of $c_0/\langle n\rangle$) found using such simple calculation (Fig. 7) is in qualitative agreement with the data in Fig. 6. In both approaches, we find that the width of spectral bands decreases slightly

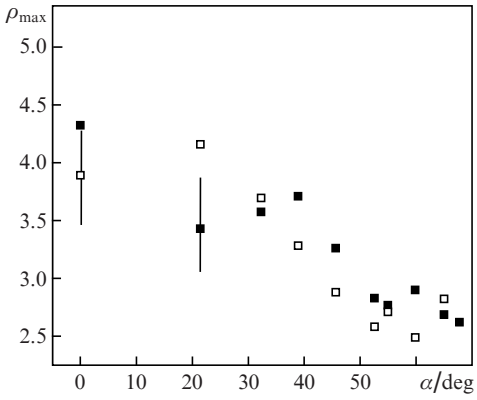

Figure 7. Angular dependences of the maximum DOS value ρ_{max} obtained for right (filled circles) and left (open circles) circularly polarised light by simulating appropriate transmission spectra.

with increasing luminescence output angle, but this causes no increase in DOS because of the larger decrease in λ^2.

5. Conclusions

In this study, we addressed an important issue pertaining to the density of photon states in CLCs: we experimentally studied light transmission and luminescence not only along the cholesteric helix axis but also at large angles to it. The CLC studied here was composed of the standard nematic mixture E7, a chiral material and a laser dye. This mixture has a well-defined photonic band gap, which shifts to shorter wavelengths as the luminescence output angle increases up to 60° in the bulk of the liquid crystal, i.e. by about 70° when the photodetector is rotated. For this purpose, a semicylindrical quartz prism was used. Using measured spectra and numerical simulation, we determined DOS spectra for polarised and unpolarised light, which characterise the structure of the CLC as a chiral one-dimensional photonic crystal.

Acknowledgements. This work was supported by the Physical Sciences Division of the Russian Academy of Sciences (basic research programme) and the Russian Foundation for Basic Research (Grant No. 11-02-00899-a).

References

1. Belyakov V.A., Sonin A.S. *Optika kholestericheskikh zhidkikh krustallov* (Optics of Cholesteric Liquid Crystals) (Moscow: Nauka, 1982).
2. Blinov L.M. S*tructure and Properties of Liquid Crystals* (Dordrecht: Springer, 2010; Moscow: LIBROKOM, 2012).
3. Palto S.P., Blinov L.M., Barnik M.I., Lazarev V.V., Umanskii B.A., Shtykov N.M. *Kristallografiya*, **56**, 667 (2011).
4. Blinov L.M., Bartolino R. (Eds) *Liquid Crystal Microlasers* (Kerala, India: Transword Research Network, 2010).
5. Kopp V.I., Zhang Z.-Q., Genack A.Z. *Prog. Quantum Electron.*, **27**, 369 (2003).
6. Schmidtke J., Stille W. *Eur. Phys. J.*, **B31**, 179 (2003).
7. D'Aguanno G., Mattiucci N., Scalora M., Bloemer M.J., Zheltikov A.M. *Phys. Rev. E*, **70**, 016612 (2004).
8. Takezoe H., Ouchi Y., Hara M., Fukuda A., Kuze E. *Jpn. J. Appl. Phys.*, **22**, 1080 (1983).
9. Lee C.-R., Lin S.-H., Yeh H.-C., Ji T.-D., Lin K.-L., Mo T.-S., Kuo C.-T., Lo K.-Y., Chang S.-H., Fuh A.Y.-G., Huang S.-Y. *Opt. Express*, **17**, 12810 (2009).
10. Palto S.P., Shtykov N.M., Umanskii B.A., Barnik M.I. *J. Appl. Phys.*, **112**, 013105 (2012).
11. Belyakov V.A., Semenov S.V. *Zh. Eksp. Teor. Fiz.*, **136**, 687 (2009).
12. Palto S.P. *Zh. Eksp. Teor. Fiz.*, **119**, 638 (2001).
13. Blinov L.M., Palto S.P. *Kvantovaya Elektron.*, **43**, 841 (2013) [*Quantum Electron.*, **43**, 841 (2013)].
14. Blinov L.M. *Pis'ma Zh. Eksp. Teor. Fiz.*, **90**, 184 (2009).
15. Palto S.P., in *Liquid Crystal Microlasers.* Eds by L.M. Blinov, R. Bartolino (Kerala, India: Transworld Research Network, 2010) pp 141–163.